Dual Contrast Cellular MRI

R. Dharmakumar[1], Z. Zhang[1], I. Koktzoglou[2], S. A. Tsaftaris[1,3], and D. Li[1,4]

[1]Radiology, Northwestern University, Chicago, IL, United States, [2]Radiology, NorthShore University HealthSystem, Evanston, IL, United States, [3]Electrical Engineering and Computer Science, Northwestern University, Evanston, IL, United States, [4]Biomedical Engineering, Northwestern University, Evanston, IL, United States

Introduction: Negative contrast MRI methods utilizing local magnetic susceptibility shifting (LMS) agents have become an active area of cellular imaging research. However, visualizing and tracking labeled cells on the basis of negative contrast is often plagued by limited specificity and/or sensitivity. Here we report on a cellular MRI method that generates a new contrast with a distinct topology for identifying labeled cells permitting significant improvement in sensitivity and specificity. Specifically, we show that FLAPS MRI [1],MRI can be used to generate fast three-dimensional images of tissue that can be rapidly processed to generate quantitative metrics enabling color overlays indicative of regions containing labeled cells.

Methods: Cell Preparation & Labeling: Acancer cell line was used throughout the study. The cells were cultured and were incubated with SPIOs (20 µg/mL, Feridex, Advanced Magnetics, USA) for 24 hrs. Unincorporated SPIOs were removed by repeated washing with PBS. Histology (Prussian blue stain) was used to confirm the cellular uptake of SPIOs and ICP-AES was used to quantify the amount of iron taken up the cells. Imaging Studies: All MRI studies were performed using a 3.0 T system (Trio, Siemens Healthcare, Germany). *(a) In-Vitro Studies:* The cell preparation was subdivided into 4 groups (4×10^6, 2×10^6, 1×10^6, 0.5×10^6), placed into Ependorf tubes,centrifuged, placed in a warm water bath and scanned individually. This was repeated 6 times to assess reproducibility. Following scout scans, bSSFP and GRE sequences were prescribed. Imaging parameters for bSSFP: spatial resolution (SR) = 0.8x0.8x1.5 mm^3;TE/TR=2.4/4.8 ms; flip angle (FA)=30°. Imaging parameters for GRE: SR=1.2x1.2x1.5 mm^3; TE/TR=10/100 ms; FA=25°. (b) *Ex-Vivo Studies:* Four SPIO-labeled cell preparations (10^6 each) were injected into fresh muscle (chicken breast). Each cell preparation was injected at 3 different locations. This procedure was repeated in 4 different pieces of tissue. Each muscle sample containing the labeled cells was immersed in standard saline bath and imaged. 3D FLAPS and GRE imaging was performed on each *ex-vivo* preparation. Scan parameters for 3D FLAPS imaging: SR=0.4x0.4x0.4 mm^3; TE/TR=2.4/4.8 ms; FA=5°. The scan parameters for the 3D GRE scans were the same, except for the following: TE/TR=10/100 ms; FA=25°. *In-Vivo Studies:* Two Wister rats were studied using the protocol and procedures approved by our institution. Labeled ($1x10^6$) and unlabeled ($1x10^6$) cells were injected into the contra-lateral hind limb muscles of the rats and 3D GRE and FLAPS acquisitions were prescribed;GRE scan parameters: SR=0.8x0.8x0.8 mm^3; TE/TR=40/2000 ms; FA=15°. FLAPS scan parameters were the same, except: SR=0.4x0.4x0.4mm^3; TE/TR=2.55/5.10 ms; FA=5°. Data Analysis: *In vitro* images were analyzed to obtain quantitative information, while *ex-vivo* and *in-vivo* data were used for qualitative evaluation of the image contrast that can be generated in tissue containing SPIO-labeled cells. For in-vitro studies, two complementary metrics were used to assess the contrast differences for each cell preparation: (1) gCNR and (2) *LC*. gCNR was defined as the mean intensity difference between bright pixels and adjacent background normalized by image noise, while *LC* was computed as the mean intensity difference between bright and dark pixels normalized by the standard deviation of the background intensity, accounting for the number of bright, dark, and background (iso-intense) pixels. Student's *t*-test was used to identify statistically significant differences in LC between the GRE and FLAPS images. Nonlinear regression analysis was performed between the estimated number of cells (N) and the contrast metrics (gCNR and *LC*). Local Contrast Sensitivity (LCS), a measure of the sensitivity of the FLAPS and GRE methods for identifying the N, was defined as the first derivative of the LC with respect to N. *Ex-vivo* and *in-vivo* FLAPS images were processed using a non-linear filter (DCIF) designed to locate SPIO-labeled cells on the basis of their dual contrast appearance.

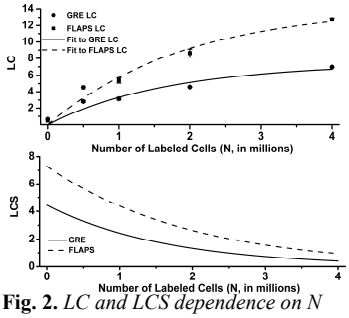

Fig. 2. *LC and LCS dependence on N*

Results: *In-Vitro Studies:* Light microscopy of the Prussian blue staining of labeled cells from various samples showed approximately 100% labeling efficiency. The iron content per cell (determined from ICP-AES): 4.75±0.11 (labeled group) vs 0.19±0.01 (control group), reported as mean±SD in pg Fe/cell. FLAPS acquisitions of SPIO loaded cells were visualized as regions of central signal voids confined by regions of positive contrast, while the GRE images were visualized as signal voids only. Paired t-test showed that, at every N, the LC from FLAPS was significantly greater than that from GRE images ($p<0.001$). LCS computation for FLAPS and GRE showed that the FLAPS LCS was nearly 2 times larger than that of GRE LCS over the range of N ($0 < N \leq 4x10^6$); refer to Fig. 1. *Ex-vivo Studies:* Visualization of the labeled cells within skeletal muscle with 3D GRE and FLAPS MRI was always possible, although the contrast characteristics between the two acquisitions were markedly different. GRE images depicted the presence of labeled cells as hypo-intense zones, while the FLAPS images showed the same regions as smaller hypo-intense regions surrounded by hyper-enhancement. When the GRE and FLAPS images were processed using DCIF, GRE images yielded negligible DCIF output values while the FLAPS images identified the regions containing the labeled cells with substantial DCIF output values (Fig. 2). Note that in the GRE image there is significant enlargement ('blooming') of the hypo-intense regions that markedly reduces the regional specificity of the cells; this effect is not observed in the FLAPS image. *In-Vivo Studies:* Labeled and unlabeled cells injected into the hind limbs of the rats were visualized on GRE and FLAPS images. On the GRE images, the unlabeled and labeled cells appeared dark, albeit the labeled cells were significantly darker. On the FLAPS images, the unlabeled cells appeared as a slightly dark zone surrounded by weakly bright pixels, and the labeled cells appeared as a substantially dark core surrounded by intense brightness. DCIF applied to the GRE image produced negligible DCIF contrast, while the FLAPS image generated marked DCIF values in the region of labeled cells and minimal DCIF enhancements in the region of unlabeled cells (Fig. 3). Note that in the GRE image, it is difficult to identify regions containing labeled cells on the basis of signal voids alone since there are several non-specific dark zones within the image that are unrelated to the labeled cells. Also note that the regional brightness in the tissue-air interface in (C) is correctly not enhanced.

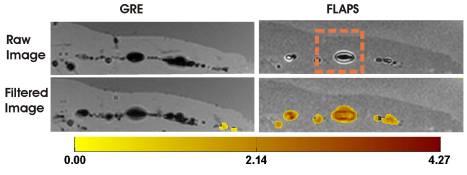

Fig. 3. *GRE and FLAPS images (top panel) and the corresponding DCIF processed images (directly below) for ex-vivo tissue with containing labeled cells. Color bar shows the value of DCIF output.*

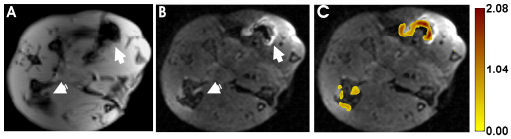

Fig. 1. *Axial GRE (A), FLAPS (B), DCIF processed FLAPS images from a rat with unlabeled and labeled cells injected in contra-lateral hind limbs. Color bar shows the value of DCIF output.*

Discussion & Conclusion: The key findings from this study were: FLAPS MRI (1) provides a unique signature to identify cells labeled with LMS agents such as SPIOs; (2) it offers nearly a two-fold increase in sensitivity to the GRE (standard) method; and (3) has the potential to improve the regional specificity of the cells compared to the standard (GRE) methods by significantly reducing the undesirable blooming artifact. Further studies are required to evaluate whether the DCIF output can be used to quantify the number of labeled cells.

References: [1] Dharmakumar *et al.* Phys Med Biol 2006.